Formability and Strength of Friction-Stir-Welded Aluminum Sheets

M.P. MILES, B.J. DECKER, and T.W. NELSON

Friction stir welding was investigated as a viable process for joining thin aluminum sheets in order to manufacture tailored blanks. In the present study three alloys were tested: 5182-O, 5754-O, and 6022-T4. All three of these alloys are being used to fabricate stamped automotive parts. The gas tungsten arc welding process has been used to make aluminum-tailored welded blanks industrially, so results using this process were compared to FSW results. Blanks of the same gage of all three alloys were welded and then evaluated using tensile and formability testing. The 5xxx series alloys had similar tensile ductility and formability regardless of the welding process. However, the 6022-T4 sheets joined using friction stir welding had better formability than those joined using gas tungsten arc welding because friction stir welding caused less softening in the heat-affected zone.

I. INTRODUCTION

THE use of tailor welded blanks (TWBs) in the automotive industry has risen substantially in the last five years, in an effort to decrease vehicle weight and improve fuel economy.[1,2,3] A TWB consists of two or more sheets of different gages, grades, or surface treatments joined together and then formed to create a part with optimal properties. For example, thicker or specialized material can be used where strength, ductility, or some other property is needed, and thinner, or nonspecialized material where specifications are not as strict. The overall stiffness of these blanks is typically better than that of conventional reinforced structures, providing an opportunity to downgage these parts,[4] particularly for aluminum alloys, where there is a cost penalty over steel. The TWBs have been fabricated using neodymium : yttrium aluminum garnet (Nd : YAG) laser welding,[5–8] mash seam welding,[5] nonvacuum electron beam (NVEB) welding,[6] and gas tungsten arc welding[2,8,9] depending on the alloy. Even with an added joining process, the weight reduction from using TWBs can be sufficient to make their use worthwhile from a cost standpoint. In some automotive applications there is potential to replace steel with aluminum alloys, which have the advantages of corrosion resistance, high strength-to-weight ratio, and recyclability. However, the difficulty in using aluminum TWBs is that the weld-affected material can be the weakest area in the part, making it necessary to redesign the shape, move the placement of the weld, or increase material thickness.

The purpose of the current work is to understand and compare the mechanical behavior of friction stir welded (FSW) aluminum alloy sheets with gas tungsten arc welded (GTAW) sheets, under stretch forming conditions. Gas tungsten arc welding has been used to make TWBs and is considered a viable process not only for lab-scale experiments, but also for industrial production.[2,10] In the ideal case the ductility of the weld region of the blank will not limit its formability. The friction stir welding process has been shown to provide superior weld properties, especially in heat-treatable, thick-plate aluminum alloys.[11,12,13] Therefore, the application of friction stir welding to the joining of thin sheets was investigated and the results were compared to gas tungsten arc welding results. Same-gage sheets will be used in the current investigation to evaluate the mechanical properties of FSW blanks. Development of tooling and process parameters for welding dissimilar-gage sheets is planned for future efforts.

M.P. MILES, Assistant Professor, Manufacturing Engineering Technology, and T.W. NELSON, Associate Professor, Mechanical Engineering, are with Brigham Young University, Provo, UT 84602. Contact e-mail: mmiles@byu.edu B.J. DECKER, formerly Graduate Student, Manufacturing Engineering Technology, Brigham Young University, is with TrimMasters, Inc., Modesto, CA.

Manuscript submitted September 12, 2003.

II. EXPERIMENTS

A. *Materials*

Three aluminum alloys were used in the present study: 6022-T4 (2.03 mm), 5754-O (1.98 mm), and 5182-O (2.03 mm). The compositions for these alloys are shown in Table I. These alloys are being developed for use in automotive stamped parts and are therefore candidates for use in tailored blank applications, where weld strength and ductility are essential. The 5182-O and 5754-O alloys are both in the annealed condition and, as a result, they strengthen significantly with the cold work that occurs during the forming process. The 5xxx series alloys are used primarily for inner body panels. The 6022-T4 alloy is partially hardened and is formable enough to manufacture stamped parts. One of the main applications for this alloy is exterior body panels, which are painted and then baked. The paint-baking process artificially ages this alloy to the T6 condition, which doubles the yield strength of the final part compared to the initial T4 condition.

B. *Welding Experiments*

Same-thickness sheets of each alloy were welded together using both friction stir welding and gas tungsten arc welding. This approach was used in order to study and compare the properties of the weld area for each process. Welding of dissimilar gages is not done in the current work, but is planned for future efforts.

The FSW samples were welded at feed rates of 13 to 60 cm/min and at speeds of 1220 to 1500 rpm. Tooling was made on

Table I. Compositions of Aluminum Alloys 5182, 5754, and 6022

Alloy	Si	Fe	Cu	Mn	Mg	Cr	Zn	Ti
5182	0.20	0.35	0.15	0.20 to 0.50	4.0 to 5.0	0.10	0.25	0.10
5754	0.40	0.40	0.10	0.50	2.6 to 3.6	0.30	0.20	0.15
6022	0.8 to 1.5	0.05 to 0.20	0.02 to 0.10	0.02 to 0.10	0.20 to 0.70	0.10	0.25	0.15

a CNC lathe from H13 tool steel, a secondary-hardening tool steel. Tools were solution heat treated at 1000 °C for 13 minutes and then were removed from the furnace and allowed to air cool to room temperature. The tempering and secondary-hardening treatment was performed at 530 °C for 1 hour. Finally, the tools were air cooled and oxide was removed. The friction stir welding parameters for the welding experiments, such as tool tilt angle, feeds, and speeds are displayed in Table II. A rendering of the tool used for the friction stir welding experiments is shown in Figure 1.

Gas tungsten arc welds were produced at a feed rate of 114 cm/min. Operating parameters were 50 pct AC at 200 Hz and 195 amps. In contrast to the friction stir welding experiments, where two blanks were welded together, the gas tungsten arc welding experiments were simplified by using full-penetration bead-on-plate welds. This approach avoids the use of filler for the 6022 alloy; at the same time, it simulates the fusion zone that would occur in a normal butt weld. The results from the bead-on-plate welds are not the same as a butt weld made with filler metal, but could be considered a best-case scenario for the gas tungsten arc welding process, especially for the 6022 alloy, where lower-strength filler metal is often used to avoid cracking in the weld.

C. *Microhardness Experiments and Metallography*

Transverse samples were removed from representative welds for microhardness and metallographic evaluations. The heat-sensitive 6022 samples were mounted in epoxy. All samples were polished in steps from 320-grit sand paper to 0.5-μm diamond paste. The Vickers microhardness tests were done with an 8-second dwell at 100 g. The indents were done on the exposed cross section of the weld 0.64 mm from the top and 0.64 mm between each indent. The 6022 specimens were not allowed to age naturally more than a few hours after welding before being tested at room temperature (samples were stored below 0 °C if they couldn't be tested right away).

D. *Tensile and Formability Testing*

The tensile specimens were made according to the ASTM E8 standard, with a gage width of 12.5 mm and a gage length of 63.5 mm. The samples were carefully machined using coolant to minimize heating. Welds (not including those in the heat-affected zone (HAZ)) accounted for about 10 pct of the gage length. Tensile testing was performed at room temperature at a rate of 2.54 mm/min. Fifteen specimens were tested for each case, with the rolling direction along the tensile axis, and the weld transverse to this axis.

Two tests were used for formability evaluation: the limiting dome height (LDH) test and the Ohio State University (OSU) test. The specimens for both LDH and OSU testing were similar, with both the weld and the rolling direction along the major axis of the specimen (Figure 2). The root side of the weld was facing in, against the punch, for all tests performed.

Table II. FSW Tooling and Process Parameters

Shoulder diameter	10.2 mm
Tool tip diameter	1.78 mm
Tool material	H13 steel
Weld speed	13 to 60 cm/min
Rpm	1220 to 1500

Fig. 1—Rendering of threaded tool used for FSW experiments.

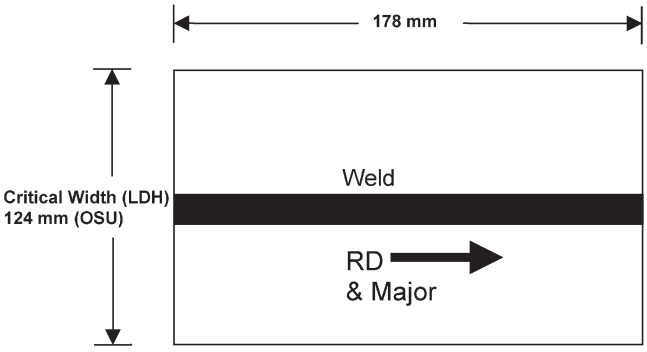

Fig. 2—Specimen used for LDH and OSU tests, with the weld and the rolling direction along the major axis of the specimen.

The LDH test is well known and has been used in industry for many years as way to measure sheet metal formability.[14] This test employs a 101.6-mm-diameter spherical punch with a set of dies that prevent draw-in and assure a pure stretch condition. The sheet is stretched to failure and the dome height is taken as the punch travels at peak load. Specimens were

degreased, deburred, and lightly coated with mineral oil. The dies were also cleaned and lightly lubricated before each test. The welded samples were positioned with the top of the weld facing out so that the punch made contact with the root side of the weld. Welds were parallel to the rolling direction and along the major axis. For all tests the clamping force was 27,200 kg and the punch speed was 1.2 mm/s. Specimens with different widths were used to find the critical width, resulting in a minimum dome height for each alloy and for each type of weld. The LDH test requires this critical-width-finding procedure for each case; sheets with different properties will have different critical widths, affecting the amount of minor strain that is produced during the test. In most cases the critical blank width produces zero, or close to zero, minor strain at the fracture location in the sheet. Once the critical width was found, 3 to 5 blanks were run to season the dies and then ten samples at the critical width were tested. For example, the base 5xxx series alloys had critical widths of about 115 mm, while the welded (both GTAW and FSW) specimens had critical widths of 124 mm. The critical width for the base 6022 alloy was 120 mm, while for the welded 6022 it was a fully-clamped specimen (178 mm). The average of ten tests was taken to determine the LDH.

The OSU test employs a cylindrical punch designed to assure stable plane-strain deformation and failure.[15,16] This test is somewhat easier to perform than the LDH test, because a critical-width-finding procedure is not required in order to obtain a plane-strain condition, making it a good choice for rapid evaluation of plane-strain stretch formability.[15] Test specimens were 178 mm long and 124 mm wide, with the weld parallel to the rolling direction and along the major axis of the specimen. Samples were degreased and deburred before they were wiped with a light application of mineral oil. Eight tests of each base alloy and of each welded alloy were averaged to evaluate formability.

E. *Forming Limit Diagrams*

A forming limit diagram (FLD) is a plot of major-*vs*-minor strain in the plane of the sheet, for different strain ratios.[17,18,19] At each minor strain there is a limiting major strain that can be achieved before failure. The locus of points for different ratios of limiting major strain/minor strain is the forming limit curve (FLC), and represents a boundary below which "safe" ratios of major-to-minor strain exist.

In order to measure surface strains, grid circles were electrochemically etched on the aluminum sheets, with diameters averaging 2.36 mm. Samples of varying widths were made up (with welds and the sheet-rolling direction along the major axis) and tested using different levels of lubrication and different specimen widths, with the LDH tooling. The different widths and lubrications resulted in different ratios of major-to-minor strain. The circles used for plotting the FLC had either no neck, an incipient neck, or a deep neck. If there was no neck, the strains were plotted as being safe; if there was an incipient or deep neck, the strains were plotted as "fail." Unwelded base sheets were used to obtain baseline FLD data for each alloy. Measurement of the major and minor axes of the circles was performed on a optical imaging machine. These measurements were used to compute true major and minor strains on each specimen, and then were plotted on the FLD.

III. RESULTS AND DISCUSSION

A. *Hardness Profiles and Microstructures*

Figure 3 shows microhardness values across friction stir welding and gas tungsten arc welding for aluminum alloy 5182-O. Alloy 5182-O is work hardenable, resulting in a slight increase in hardness through the friction stir welding due to both the significant decrease in grain size and the residual work hardening from the stirring process. In contrast, the gas tungsten arc welding profile is relatively constant from the base material into the HAZ and across the weld nugget. For alloy 5754-O, there was very little difference in the hardness profile of the GTAW and FSW specimens, as shown in Figure 4.

The results for alloy 6022-T4 are quite different. This alloy is precipitation hardenable, with a T4 temper, and loses a significant amount of strength during the welding. Although

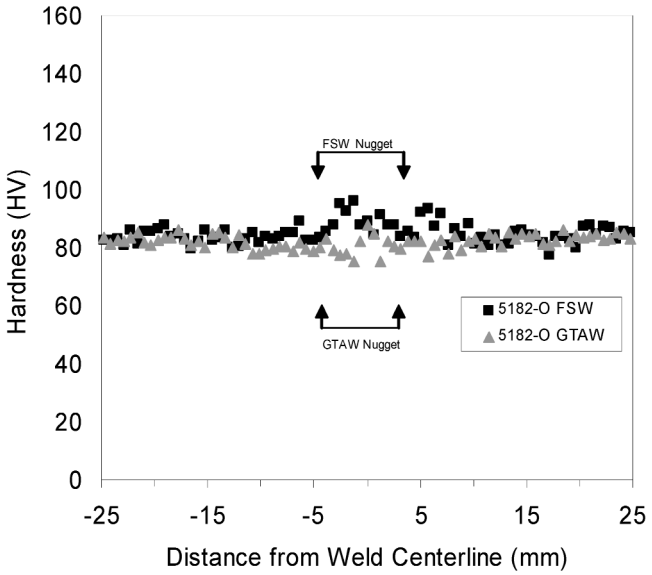

Fig. 3—Vickers microhardness profiles for FSW and GTAW, alloy 5182-O.

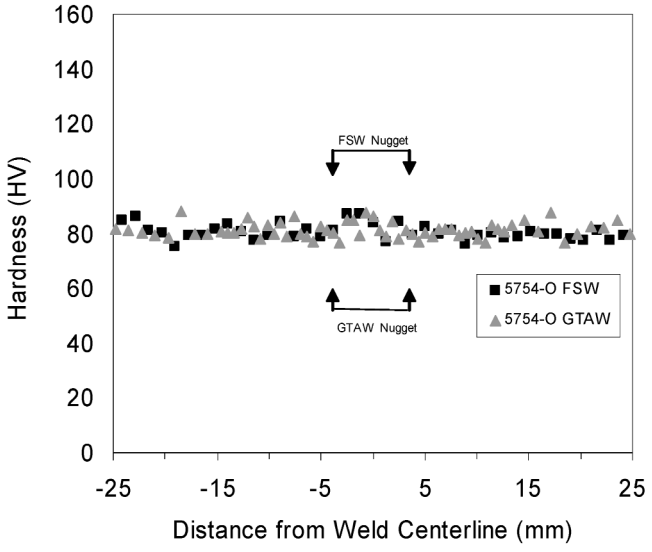

Fig. 4—Vickers microhardness profiles for FSW and GTAW, alloy 5754-O.

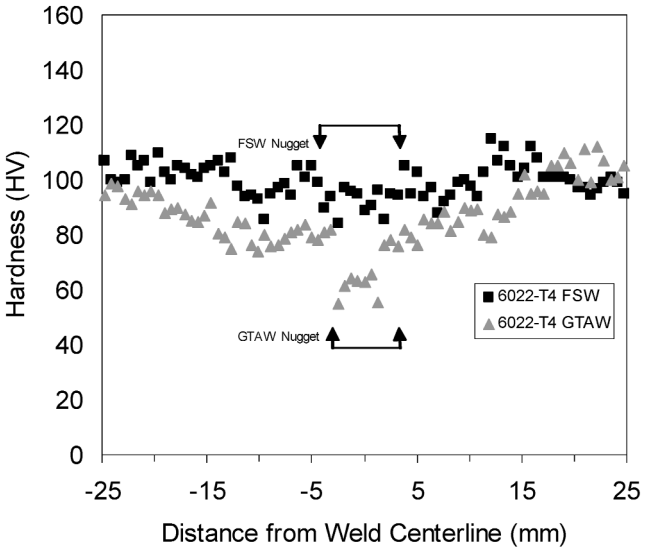

Fig. 5—Vickers microhardness profiles for FSW and GTAW, alloy 6022-T4.

there is significant softening in both cases, the FSW specimens exhibit less softening than the GTAW specimens, as seen in Figure 5.

The microstructures in the welds are similar for a given welding process (Figures 6, 7, and 8). Friction stir welding resulted in a fine, uniform grain size (usually 10 to 20 μm) in the weld nugget, with essentially no change in grain size in the HAZ adjacent to the weld. In contrast, gas tungsten arc welding produced a typical cast microstructure with large, columnar grains in the weld nugget.

B. *Tensile and Formability Testing*

A summary of the tensile data is shown in Tables III through V. For the 5182-O and the 5754-O alloys, there were no significant differences in any of the average tensile properties of the FSW and GTAW samples at the 95 pct confidence level. For 6022-T4, the yield strength and ultimate tensile strength drops significantly in the welded specimens, although the FSW specimens retain more strength than the GTAW specimens. In addition, the FSW samples had a greater average elongation than the GTAW samples, by about 50 pct. In this alloy, the fracture location was always in the HAZ for the FSW samples, while it was always in the weld for the GTAW samples. This can be explained by looking at Figure 5, where the softening in the gas tungsten arc welding case is seen to be much greater than in the friction stir welding case.

The average tensile properties for the FSW samples were more consistent than those of the GTAW samples, particularly in the case of alloy 6022-T4. While the variance in the yield strengths are similar, the ultimate tensile strength, uniform elongation, and total elongation for the FSW specimens are significantly less than those of the GTAW specimens.

The LDH results are shown in Figure 9 and the OSU results are shown in Figure 10. Again, the two 5xxx series alloys perform about the same regardless of the welding process used, while the 6022-T4 has a lower LDH for gas tungsten arc welding than for friction stir welding. The FSW

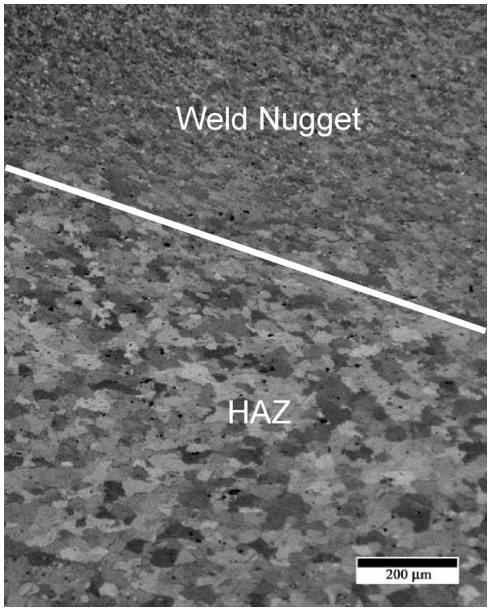

(*a*)

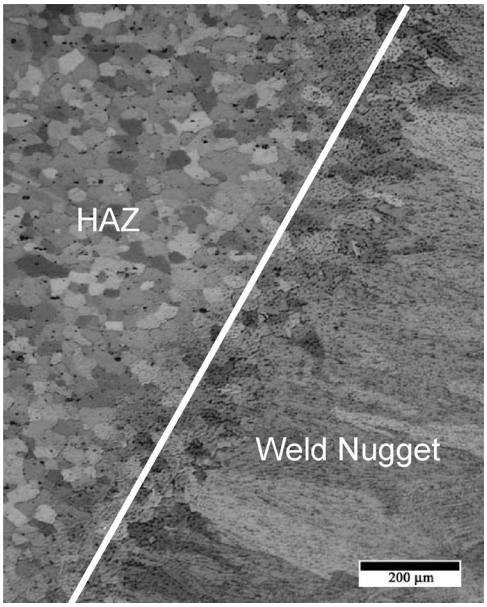

(*b*)

Fig. 6—Transition between the weld nugget and the HAZ in alloy 5182-O for (*a*) FSW and (*b*) GTAW. The FSW weld nugget has a fine grain size (10 to 20 μm), while the GTAW nugget has a classic cast microstructure.

specimens failed in the HAZ and not in the weld for the LDH test, but several of the GTAW samples failed in the weld. For the 6022-T4, the differences between the friction stir welding and gas tungsten arc welding results are not as great when the OSU test was performed. This is because the OSU test causes stretching along the weld but not across it, resulting in a plane-strain fracture perpendicular to the weld (and to the major strain direction), as shown in Figure 11. On the other hand, the full-dome LDH test causes stretching both along and across the weld. The strain applied across the weld and the HAZ causes deformation to localize in this softened region, creating a fracture parallel to the weld

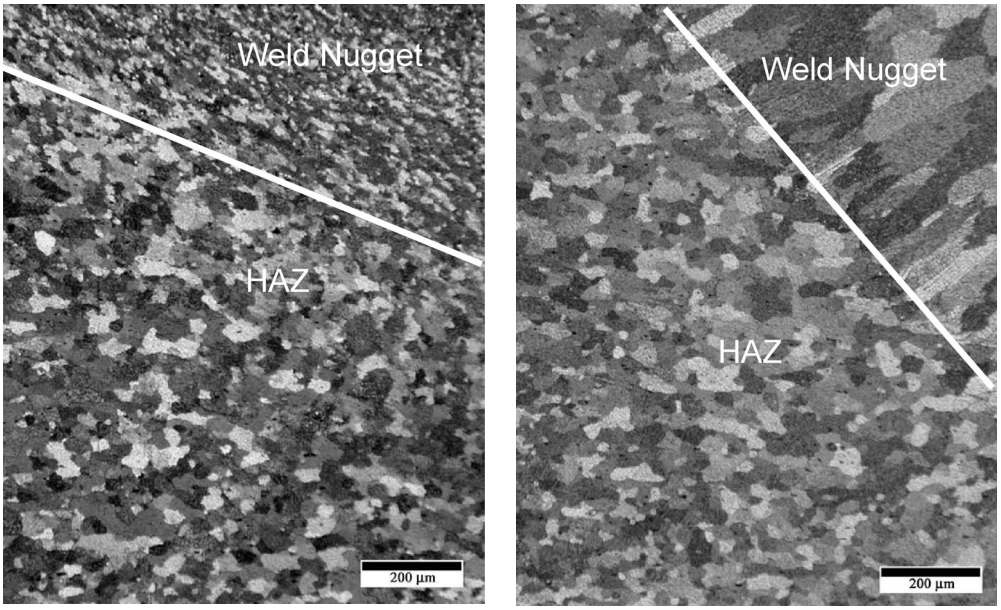

(*a*) (*b*)

Fig. 7—Transition between the weld nugget and the HAZ in alloy 5754-O for (*a*) FSW and (*b*) GTAW. The FSW weld nugget has a fine grain size (10 to 20 μm), while the GTAW nugget has a cast microstructure.

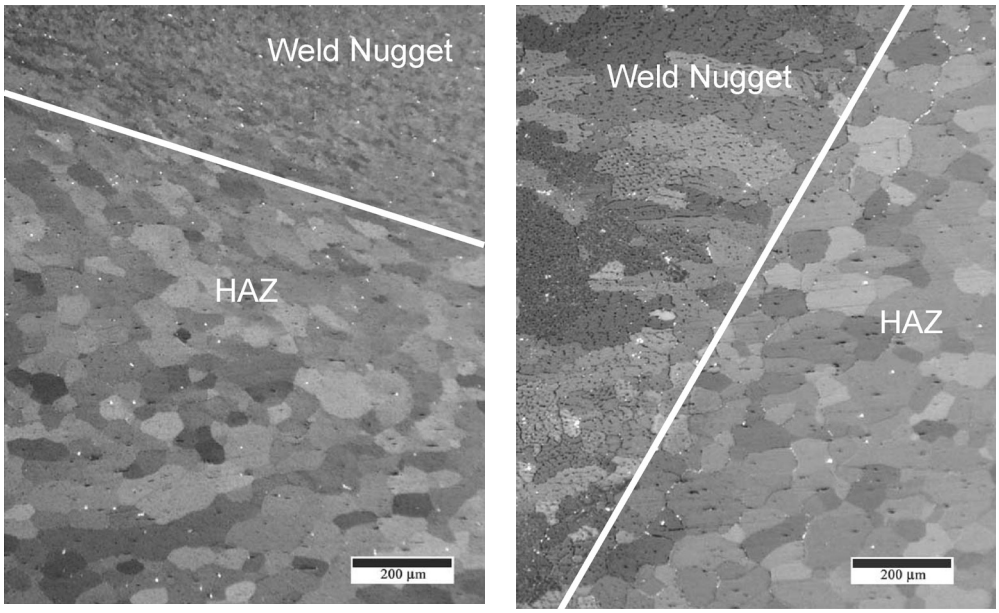

(*a*) (*b*)

Fig. 8—Transition between the weld nugget and the HAZ in alloy 6022-T4 for (*a*) FSW and (*b*) GTAW. The FSW weld nugget has a fine grain size (10 to 20 μm), while the GTAW nugget has a cast microstructure.

Table III. Tensile Data for Base and Welded 5182-O Sheets

Weld Type	0.2 Pct Yield (MPa)	UTS* (MPa)	Elongation at UTS	Total Elongation	Fracture Location B = Base H = HAZ W = Weld	Number of Samples
Base	131.0	285.4	25.3 pct	27.3 pct	N/A	15
Standard deviation	2.2	3.3	0.1 pct	0.7 pct	—	—
FSW	138.2	285.7	23.3 pct	25.7 pct	B = 100 pct	15
Standard deviation	4.6	1.7	0.1 pct	0.7 pct	—	—
GTAW	127.4	283.2	24.9 pct	27.0 pct	B = 100 pct	15
Standard deviation	5.5	2.1	0.2 pct	1.0 pct	—	—

*UTS—ultimate tensile strength.

Table IV. Tensile Data for Base and Welded 5754-O Sheets

Weld Type	0.2 Pct Yield (MPa)	UTS (MPa)	Elongation at UTS	Total Elongation	Fracture Location B = Base H = HAZ W = Weld	Number of Samples
Base	94.4	236.3	24.6 pct	26.5 pct	N/A	15
Standard deviation	4.3	5.6	1.5 pct	1.0 pct	—	—
FSW	98.1	235.6	22.7 pct	24.9 pct	B = 100 pct	15
Standard deviation	6.3	2.5	1.0 pct	0.8 pct	—	—
GTAW	96.6	235.5	22.1 pct	24.1 pct	B = 100 pct	15
Standard deviation	2.0	5.6	1.7 pct	2.0 pct	—	—

Table V. Tensile Data for Base and Welded 6022-T4 Sheets

Weld Type	0.2 Pct Yield (MPa)	UTS (MPa)	Elongation at UTS	Total Elongation	Fracture Location B = Base H = HAZ W = Weld	Number of Samples
Base	163.6	263.3	26.3 pct	29.6 pct	N/A	15
Standard deviation	1.9	1.2	1.0 pct	1.0 pct	—	—
FSW	140.1	235.0	12.3 pct	12.9 pct	H = 100 pct	15
Standard deviation	4.7	4.7	0.4 pct	0.6 pct	—	—
GTAW	119.7	207.4	7.7 pct	8.2 pct	W = 100 pct	15
Standard deviation	5.2	14.7	1.7 pct	1.8 pct	—	—

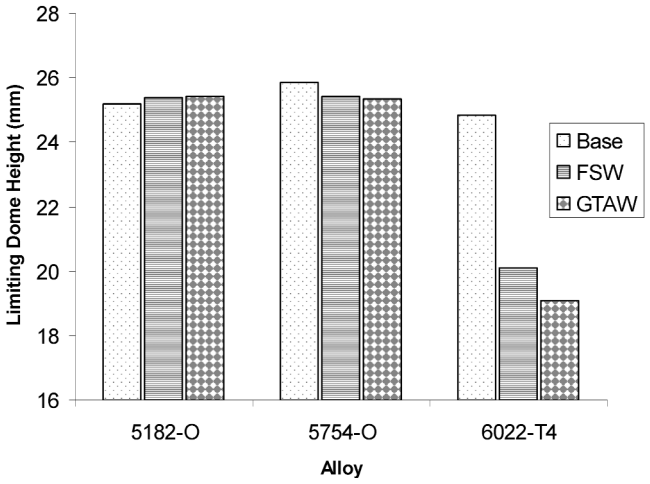

Fig. 9—LDH test results for three alloys using base sheets, FSW sheets, and GTAW sheets.

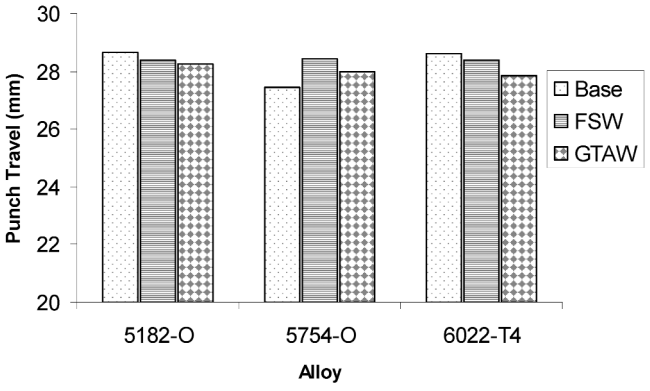

Fig. 10—OSU test results for three alloys using base sheets, FSW sheets, and GTAW sheets.

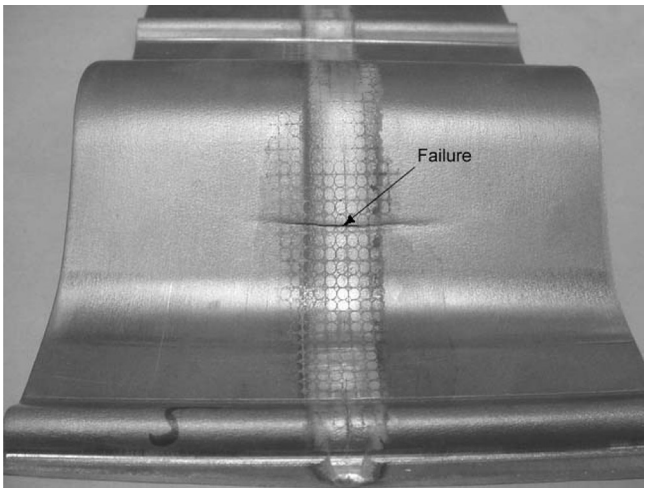

Fig. 11—Failure in alloy 6022-T4 during the OSU test occurred in about the same location, across the weld, for all tests.

(or in the weld for some GTAW specimens), as seen in Figure 12. This biaxial mode of deformation highlights the differences in weld performance between the friction stir welding and gas tungsten arc welding processes better than a plane-strain condition, when the weld is oriented along the major strain axis.

In summary, the friction stir welding process results in about the same average formability (as measured by both tensile elongation and formability testing) as the gas tungsten arc welding process for the 5182-O and 5754-O welded sheets, but with slightly more consistent properties. For the 6022-T4 alloy, friction stir welding provides better ductility than gas tungsten arc welding, because it causes less softening in the HAZ, as seen in the microhardness results. However, its advantage depends on the deformation mode imposed. When tensile stretch conditions (with the weld transverse to

the tensile axis) or biaxial stretch conditions were imposed on the weld, the FSW samples performed better than GTAW samples. When a plane-strain deformation condition was imposed (with the weld along the major axis), FSW samples did not have much advantage.

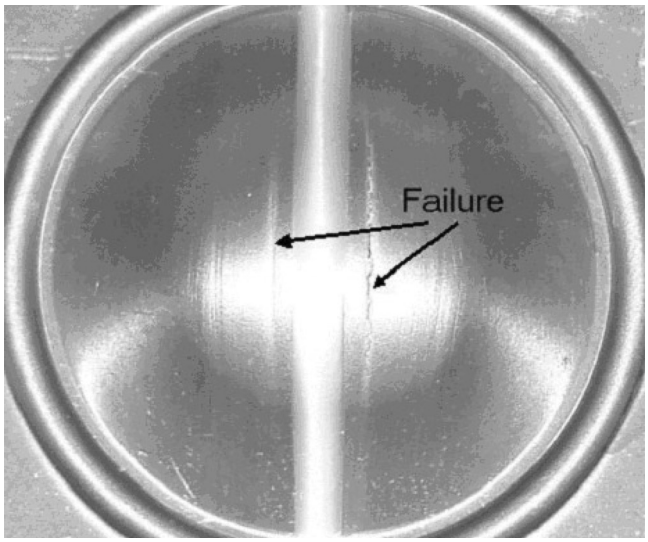

Fig. 12—Failure in alloy 6022-T4 during full dome LDH tests occurred in the HAZ, on either side of the weld, for all of the FSW specimens. For GTAW specimens, many of the failures occurred in the weld.

C. *Forming Limit Diagrams for FSW Sheets*

The ductility of FSW sheets was shown to be at least as good and in most cases superior to that of GTAW sheets, based on the tensile and formability results. Therefore, some preliminary FLD data are shown here that compare unwelded base sheets and FSW sheets. The right-hand side of the FLD (the side for which minor strains are positive) for base and welded 5182-O sheets is shown in Figure 13. While the forming limits of the base and FSW 5xxx series sheets are not far apart in plane-strain, the biaxial forming limits are higher for the base sheet material. A similar result is obtained for 5754-O, as shown in Figure 14. For the 6022-T4 alloy, the differences are more pronounced, as shown in Figure 15. The forming limits of the FSW sheets decrease rapidly as the strain ratios move toward biaxial tension. This is consistent with the formability results in Section III–C, where the lowest forming heights for FSW 6022-T4 were obtained with a fully clamped specimen that produced biaxial or near-biaxial strain states at failure.

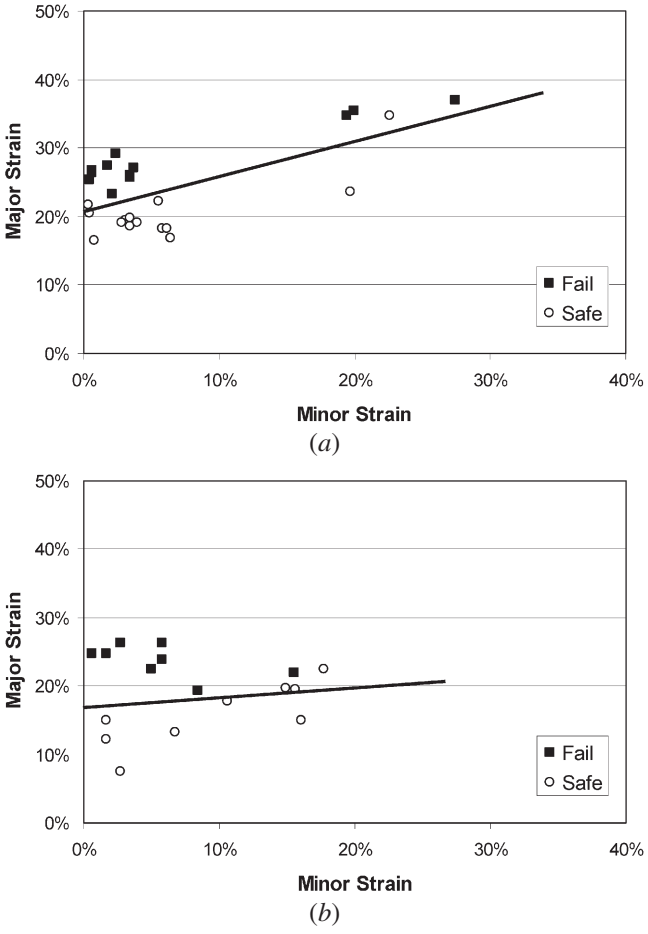

Fig. 13—FLDs for 5182-0: (*a*) base material and (*b*) FSW material.

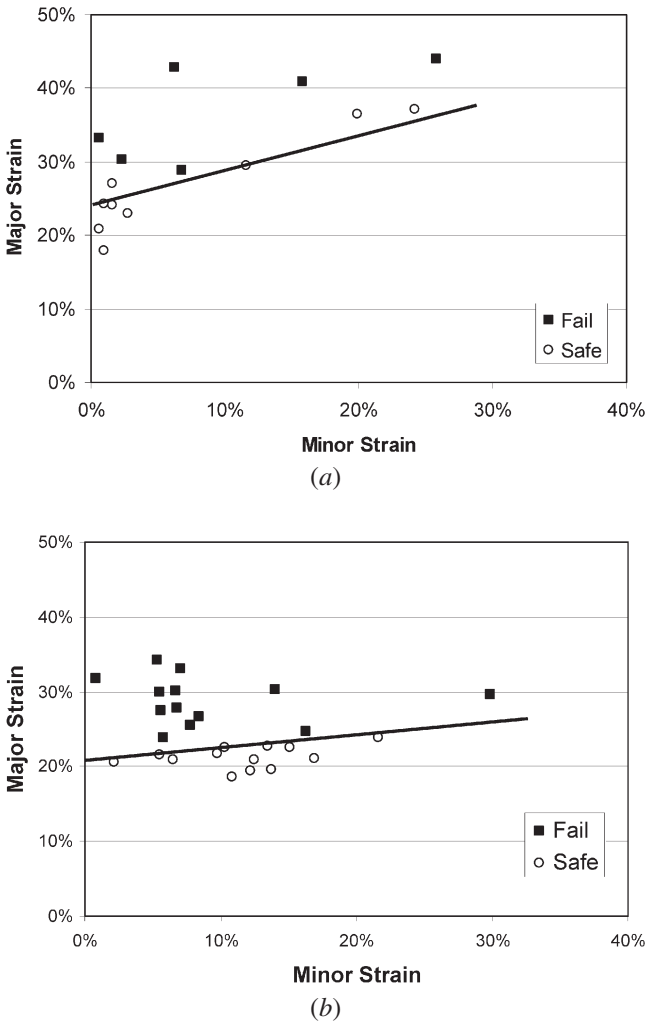

Fig. 14—FLDs for 5754-0: (*a*) base material and (*b*) FSW material.

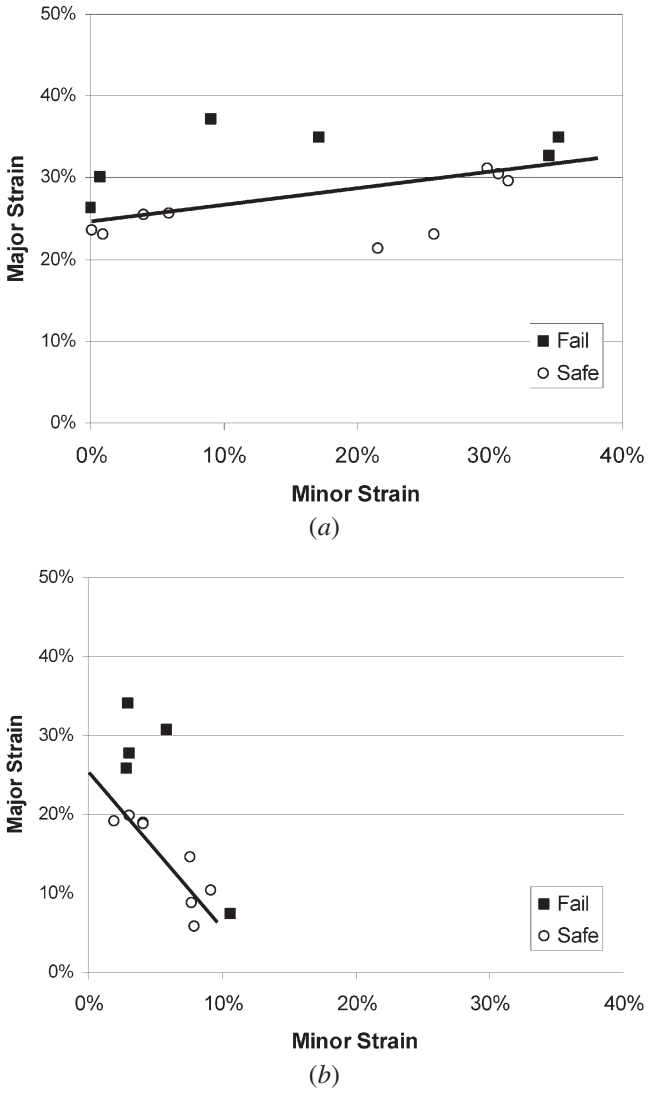

Fig. 15—FLDs for 6022-T4: (*a*) base material and (*b*) FSW material.

IV. SUMMARY AND CONCLUSIONS

The formability of welded aluminum blanks was evaluated for the friction stir welding and gas tungsten arc welding processes. Three alloys were studied: 5182-O, 5754-O, and 6022-T4. Same-gage sheets were welded together and tested in a variety of configurations and compared to unwelded base material performance. The following conclusions were drawn from the results of this study.

1. Both 5182-O and 5754-O welded sheets had similar ductility in uniaxial tension and formability testing, regardless of the welding process applied to the sheets.
2. The FSW 6022-T4 sheets retained about 43 pct of the base material tensile elongation with the weld transverse to the tensile axis and the rolling direction along the tensile axis. This result was still better than the GTAW sheets, which retained only about 28 pct of the base material elongation.
3. Formability testing showed that the FSW 6022-T4 sheets were more formable than the GTAW sheets when evaluated using full-dome LDH tests, and were slightly more formable when using OSU plane-strain tests.
4. Forming-limit diagrams for the 5182-O and 5754-O FSW sheets were similar to those of the unwelded base material near plane strain; however, the FSW sheets had lower forming limits than the base sheets as biaxial strain conditions were reached. The FSW 6022-T4 alloy also had similar formability as the base material in plane-strain, but had rapidly decreasing formability as biaxial strain conditions were approached and straining occurred across the weld.

ACKNOWLEDGMENT

The authors thank Sherri McCleary of Alcoa Technical Center for supplying the sheet alloys used for this study.

REFERENCES

1. B. Kinsey, V. Viswanathan, and J. Cao: *J. Mater. Manufacturing*, 2001, vol. 110, Sect. 5, pp. 673-79.
2. R.W. Davies, G.J. Grant, H.E. Oliver, M.A. Khaleel, and M.T. Smith: *Metall. Mater. Trans. A*, 2001, vol. 32A, pp. 275-83.
3. T. Pohl: *32nd ISATA Conf.*, June 14–18, 1999, ISATA, Croyden, Vienna, 1999, pp. 441-49.
4. P.A. Friedman and G.T. Kridli: *J. Mater. Eng. Performance*, 2000, vol. 9 (5), pp. 541-51.
5. K.K. Bhatt and M. Eisenmenger: SAE Paper No. 950923, SAE, Warrendale, PA, 1995.
6. A. Buste, X. Lalbin, and M.J. Worswick: *Proc. Int. Symp. on Light Metals*, M. Bouchard and A. Faucher, eds., Canadian Institute of Mining, Metallurgy, and Petroleum, Montreal, 1999, pp. 485-500.
7. P. Martin, R. Zhang, B. Altshuller, M.J. Finn, and M.J. Worswick: *Proc. Int. Symp. on Light Metals*, M. Sahoo and C. Fradet, eds., Canadian Institute of Mining, Metallurgy and Petroleum, Montreal, 1998, pp. 409-23.
8. M.C. Stasik and R.H. Wagoner: in *Aluminum and Magnesium Automotive Applications*, J.D Bryant, ed., TMS, Warrendale, PA, 1996, pp. 69-83.
9. F. Herrmann, J. Ebert, M. Hibben, and F. Steimmel: *Automation*, 1996, vol. 1, pp. 507-16.
10. R.W. Davies, H.E. Oliver, M.T. Smith, and G.J. Grant: *J. Met.*, vol. 51 (11), pp. 46-50.
11. L.E. Murr, G. Liu, and J.C. McClure: *J. Mater. Sci.*, 1988, vol. 33, pp. 1243-51.
12. M.W. Mahoney, C.G. Rhodes, J.G. Flintoff, R.A. Spurling, and W.H. Bingel: *Metall. Mater. Trans. A*, 1998, vol. 29A, pp. 1955-64.
13. Y.S. Sato, H. Kokawa, M. Enomoto, and S. Jogan: *Metall. Mater. Trans. A*, 1999, vol. 30A, pp. 2429-37.
14. A.K. Ghosh: *Met. Eng. Q.*, 1975, vol. 15 (3), pp. 53-64.
15. M.P Miles, J.L. Siles, R.H. Wagoner, and K. Narasimhan: *Metall. Trans. A*, 1993, vol. 24A, pp. 1143-51.
16. R.H. Wagoner, W. Wang, and S. Sriram: *J. Mater. Processing Technol.*, 1994, vol. 45, pp. 13-18.
17. S.P. Keeler and W.A. Backofen: *Trans. ASM*, 1963, vol. 56, pp. 25-48.
18. S.P Keeler: SAE Paper No. 650535, SAE, Warrendale, PA, 1965.
19. S.S. Hecker: *Sheet Met. Ind.*, 1975, Nov., pp. 671-76.